SciEn
Journal of Engineering Advancements Vol. 04(03) 2023, pp 90-100 https://doi.org/10.38032/jea.2023.03.005

A Micro Energy Grid Optimal Design and Economic Operation Using Genetic Algorithms

Ahmed S. Eldessouky [1,*] *and Abbdallah Fahmy* [2]

[1]Faculty of Energy and Environment Engineering, BUE, Cairo, Egypt
[2]Canadian International College, Cairo, Egypt

Received: May 07, 2023, Revised: August 27, 2023, Accepted: August 27, 2023, Available Online: September 29, 2023

ABSTRACT

This paper presents an optimal design procedure and economic operational scheduling of micro energy grids (MEGs). The optimization objectives are to minimize cost, carbon dioxide emissions, and energy deficiency. The energy sources and conversion technologies included in this study are renewable-based sources (wind and photovoltaic), a furnace, an electrical heater, a main power grid, and a local power station. Two proposed control levels are applied to control the operation of the MEG. The supervisor control level selects the energy supplier based on price and/or availability. The inner control level dynamically matches the demand profile with the supply profile. The control loops guarantee dynamic matching between the demand profile and supply profile. Two scenarios are simulated, zero interest rates and 5.25% interest rates. The results showed renewables contribute with a significant share as an energy source, however, higher interest rates would negatively impact this contribution. It also confirms that carbon taxes can reduce the use of fossil fuels as an energy source.

Keywords: Micro Energy Grid, Energy Grid Operation, Optimal Structure of Energy Grid, Genetic Algorithms, Renewable Energy Sources

1 Introduction

In 2019, global energy demand increased by 8.4%. However, due to renewable energy contributing to 29% of total demand growth, greenhouse gas emissions increased only by 1.4% [1]. In the previous 5 years, the greenhouse gas emissions were kept unchanged while the energy demand had increased by a rate of 1.4% [2]. This is due to the significant penetration of renewable-based energy in energy production that reduces greenhouse gas emissions caused by energy production.

A Micro Energy Grid (MEG) can integrate renewable energy sources (RESs) and distributed generators (DGs) in an energy system that satisfies the energy demand in local geographical areas [3]. MEG facilitates better control of energy production and emission, reduces power outage risk, and increases energy reliability [4]. They can utilize local energy resources with a lower dependency on centralized power plants based on their operational mode (islanded or grid-connected). Hence, power transmission loss and transmission infrastructure can be greatly reduced. The term Micro Energy Grid (MEG) was recorded in some articles to replace MG with the same definition. However, some articles use this term (MEG), with the addition of "Energy" to indicate the integration of other forms of energy rather than electricity, such as heat and gas [5],[6]. The integration of other forms of energy provides more effective and optimal solutions with the presence of more supply options. Combined heat and power (CHP) generators with heat generation are examples of supplying energy in other forms rather than electricity. Utilizing wasted energy from such resources increases their efficiency and reduces energy costs and emissions. In this paper, MEG is used to refer to the integration of different forms of energy. MEGs offer many benefits such as

1) Ability to supply growing demand with minimal modification to energy transmission infrastructure of the main grid.
2) Reduce energy loss due to energy transmission.
3) Allow local management of energy demand by load shedding/scheduling.
4) Minimize the risk of a power outage with the presence of different supply resources.
5) Reduce emissions by integrating renewables as a source of energy.
6) Deploy, maintain, and operate energy generators in an efficient manner.
7) Supply isolated areas with required energy using available local energy sources.

MEG planning and operational scheduling is a multi-objective optimization problem where size, structure, and interconnection are among different parameters affecting the optimization objectives (cost and reliability). While some research activities show interest in optimizing MEG locally [6], others focused on the interconnection options with other MEGs and the main utility network [7]-[9], reducing the operation cost by load shifting [10], or scheduling of energy storage systems [11],[12]. The mentioned work used AI algorithms in their optimization processes such as genetic algorithms [10]-[11] and fuzzy logic [12].

Moghaddam et al. [13] introduced MG optimization with local optimization objectives (ignoring the transformer losses). They applied the modified particle swarm optimization technique with adaptation capabilities to reduce optimization dependency on learning factors and momentum weight factors in conventional PSO. They adopted a time of 24 hours for the optimization process, as the algorithm is an online power

*Corresponding Author Email Address: Ahmed.eldessouky@bue.edu.eg Published by: SciEn Publishing Group

dispatch process. Sizes of DGs are assumed constant, hence, no optimization for the sizes of DGs greatly affects the initial cost.

Díaz et al. [14] developed an optimal energy policy for MG in a grid-connected mode under uncertainty. They considered wind turbines (WT) and gas microturbines as hybrid power systems, in addition to the main grid. Levelized Cost of Energy (LCoE) is used as an objective function for connection policy. The operation expenditures, gas, and electricity prices (OPEX), together with capital expenditures (CAPEX), are used to find the optimal policy for switching between gas microturbine and main grid to compensate for energy deficiencies between demand and WT generation. Their work considers the uncertainty of prices, not energy availability. The CAPEX for grid connectivity was not included. The authors developed the Ornstein-Uhlenbeck (OU) process, which satisfies the stochastic differential equation model to present the uncertainty of both price and load. Another work on optimal energy management under uncertainty can be found in [15]. Katzenbach et al. [8] developed a methodology for energy conservation and resource management in building systems. Their work focused on listing sequential procedures to examine the effectiveness of different energy options. Kouloura et al. [16] presented a methodology for decomposing energy problems for buildings into multi-energy systems in different forms (hyper, parallel, and sub-systems). The methodology allows us to observe the coupling of energy processes in buildings, based on the system analyses of student housing buildings in the city of Xanthi, Greece, as a case study. They proposed a set of interventions to improve energy consumption, cost, and emission. No optimization algorithm is used, and only human knowledge and experience are used for energy optimization measures and evaluation. Zidan et al. [17] presented optimal deployment of distributed generation (DG) based on capacity sizes and types. They assume a static model of energy generators and storage. Hence, only open-loop control was used in their algorithm.

In this paper, an optimal structure and economic operation of MEG is performed. The MEG operation and scheduling are performed by applying two control levels. The upper control level (supervise controller) provides optimal operation of MEG, based on fuel prices and availability, to satisfy the load demand. While energy prices can be easily achievable, the availability of energy from each source is not. In the previous work, the operation and optimization algorithms assume unlimited energy sources, neglecting the limited structure of MEG. In addition, they either neglect the losses of energy generators and converters or consider them as static losses. Hence, their work lacks practicality.

This paper provides a significant contribution by accounting for limited energy sources, and the dynamics of power loss of each component in the MEG. As the losses of different components of MEG are dependent on the load value, they can't be presented as static values. Hence, a lower-level dynamic control process (PI algorithm) was adopted to satisfy dynamic heat and power load in the presence of dynamic losses of energy conversion technologies, and power limitation of those sources. Once the lower control level signals no availability to supply the required power from a selected source, the upper control level shifts demand to the second lower-cost power source. Moreover, the paper accounts for the presence of local power stations that can export surplus energy with prices lower than the prices of the main grid.

With the implementation of two-level control loops to MEG under consideration, an optimal operation is guaranteed; however, it doesn't guarantee its optimal structure. Therefore, genetic algorithms (GA) are implemented to find the optimal structure of the MEG under its optimal operating conditions. Annual capital expenditure, maintenance, operation (M&O) expenditure, emission, and energy deficiency are used to form objective functions for the optimization process. The MEG is designed to supply a small-sized town of 200 midsize houses, located near urban Toronto, Ontario Canada (Heat and power loads).

The paper is organized as follows: Section 2 describes the MEG structure. Each energy source model is presented in the subsections of Section 2. The models included the economic model (annual capital expenses and operation expenditure), the generation model for renewable sources, and the losses model for other energy sources. Section 3 discusses the control algorithm. Section 4 introduces the optimization algorithm. Section 5 presents the simulation process and discusses the results. Finally, the conclusion is presented in Section 6.

2 MEG structure

The proposed MEG structure is shown in Fig. 1. It is composed of renewable sources (wind turbine and PV array), a gas furnace, an electrical heater, and a step-down transformer. The structure assumes direct supply from private/local stations, with the same operating voltage levels of the load (no transformer is required). The MEG is connected to the main grid via a step–down transformer for importing/exporting power from/to the grid. Its model presentation in the simulation is essential for cost and power loss calculations.

It is assumed that heat generation from the furnace is dependent only on furnace capacity and required heat energy. The gas supply to the furnace is assumed to be unlimited. The system is composed of two coupled control loops, one for the power and one for the heat. The required power is satisfied, first, by the renewables. If renewables don't satisfy the required power, a controller requests additional power from the main grid or the private local station, based on price and availability. If renewables produce power greater than required, the heat controller will direct surplus power to satisfy the required heat. If surplus power doesn't satisfy the required heat, the heat controller satisfies the missing heat either from the furnace or from the electrical heater, according to the price and capacity of the furnace and electrical heater. Any surplus energy from renewables, after satisfaction of power and heat requirements, will be exported to the main grid via the utility transformer.

Fig. 2 shows the structure of the two-level control system applied to the MEG. The supervisor controller represents the upper control level at which it determines the required power that should be supplied from each source. The amount of required power from each source is determined based on price and availability. The availability is a feedback signal generated by the source model. This signal is dynamically changed according to current power generation, power losses, and the source capacity (green dashed line in Fig. 2).

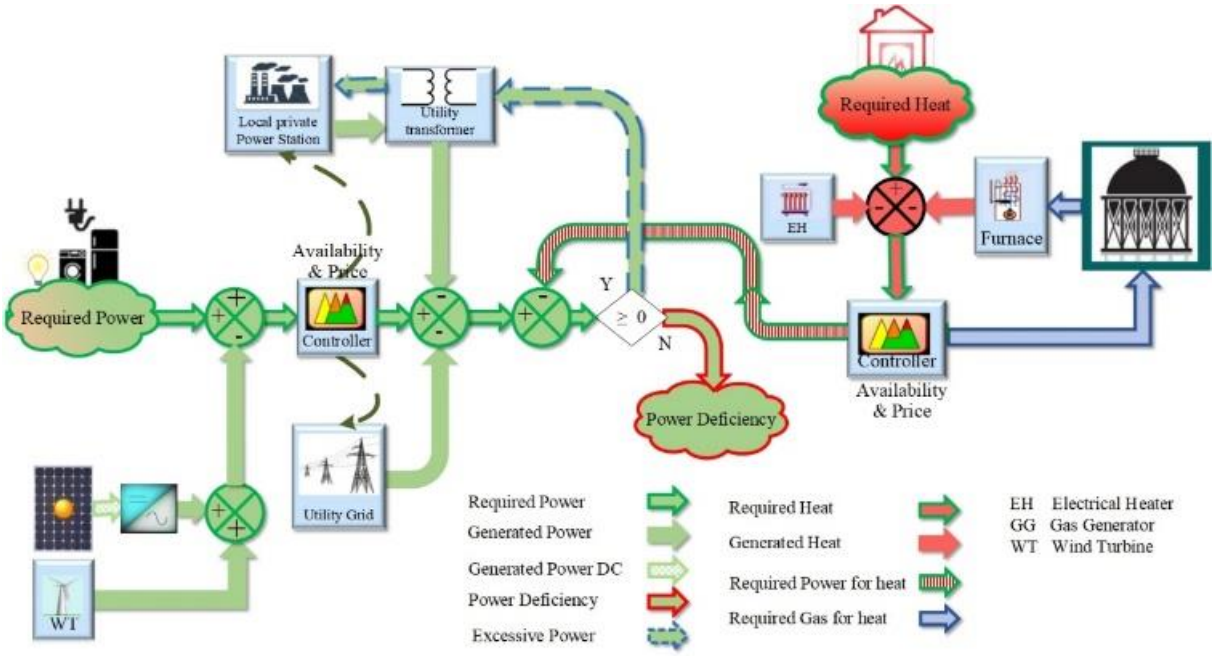

Fig. 1 The proposed MEG structure

The lower control level is a PID algorithm applied for each energy source. It ensures that the source produces the required amount of power, provided that the limits of the source, according to its capacity, were not reached. If the generated power and power loss reach the limits of source capacity, the model signals zero availability to the supervisor controller to shift demand to the next available sources.

The following subsections describe the economic and power models of each energy source.

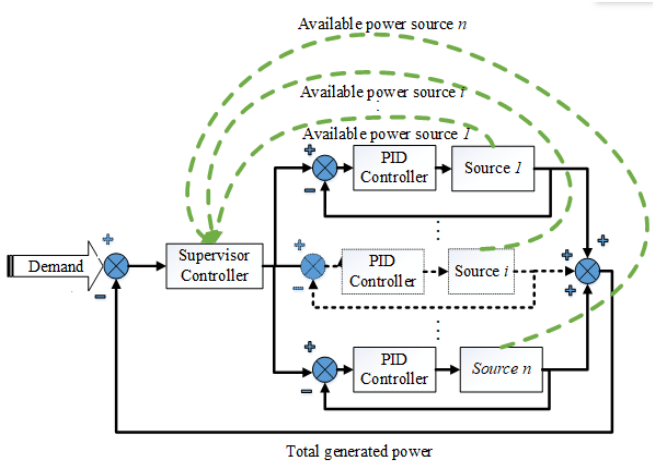

Fig. 2 Two-level Control MEG

2.1 Wind turbine model

Wind turbines (WTs) are among the renewable technologies that have a high penetration rate in MEGs. The global wind power capacity increased from 48,000 MW in 2004 to 370,000 MW in 2014 with a growth rate of 16% in 2014 [2]. In 2019, the total world generation of wind energy increased to 651 GW [1]. Annual wind capacity additions declined by 21% from 2021 to 2022 due to delayed wind projects in China caused by Covid-related restrictions. However, it is expected to rebound by 70% addition in 2023 [18], Due to the limited production time of PV systems (during daytime only), WTs provide an alternative renewable source that can produce power independent of the time of day, but rather depending on the wind power availability at a given time. The wind power (P_{wind} (kW)) at a given wind speed (v (m/s)) can be determined as follows:

$$P_{\text{wind}} = {}^{1}/_{2}\,\rho R v^{3}/1000\ kW \quad (1)$$

where is the air density (nearly 1.225 kg/m^2 $at\ sea\ level$) and R is the radius of the wind rotor. The relation between wind power and wind turbine output power is given by:

$$P_{\text{WT}} = P_{\text{wind}} \times \left(\frac{16}{27}\right) \times C_P \quad (2)$$

Where 16/27 is the Betz limit and C_P is the Turbine capacity. Turbine efficiency was set to 30 % [4] hence, at a wind velocity of 14 m/s, the wind turbine can generate a peak power of 504 W/m^2.

Besides its capital cost and size, the wind power curve is the main characteristic of WT that plays a major role in its selection. A linearized wind power curve is used in this study as shown in Fig. 3 [4].

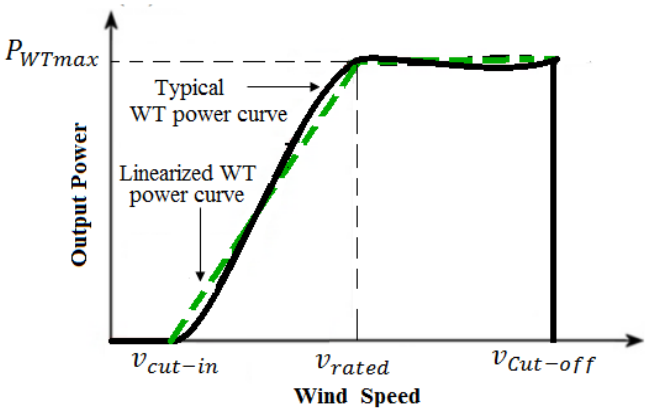

Fig. 3 Typical and linearized wind turbine output power with wind speed curve

According to the trend shown in Fig. 3, the output power of wind turbine is given by [19]:

$$P_{WT}(k)=\begin{cases}0 & v(k)<v_{in}\\ \frac{P_{WTr}}{v_r-v_{in}}\times(v(k)-v_{in}) & v_{in}\le v(k)\le v_r\\ P_{WTr} & v_r\le v(k)\le v_{off}\\ 0 & v(k)>v_{off}\end{cases} \quad kW \qquad (3)$$

Where $P_{WT}(k)$ is the generated power of the WT at wind speed $v(k)$, v_{in} is the cut-in wind speed, v_r is the wind speed at which WT generate power at its rated power (P_{WTr}), and v_{off} is the wind speed at which the WT braking system is activated to avoid WT mechanical failure. Further details on the dynamic model of the wind turbine can be found in [7].

The annual generated energy by WT is given by:

$$E_{WT}=\sum_{k=1}^{8760}P_{WT}(k) \qquad kWh \qquad (4)$$

The capital cost of different-sized WT is given in Table 1.

Table 1 Wind turbine cost base on size [1],[20].

Size	Cost ($/kW)
1kW turbine	10,000
5kW turbine	5,000
250kW turbine	3,500 -2,500

The capital cost of WT can be calculated as follows:

$$C_{CaWT}=\alpha_{WT}\times P_{WTnom} \qquad (5)$$

where α_{WT} is the cost of WT per kW, and P_{WTnom} is the nominal power of installed WT. α_{WT} can be calculated as follows:

$$\alpha_{WT}=\begin{cases}\alpha_{WT_1} & P_1\ge P_{WTnom}\\ \vdots & \vdots\\ \alpha_{WT_i} & P_i\lesssim P_{WTnom}\lesssim P_{i+1}\\ \vdots & \vdots\\ \alpha_{WT_N} & P_N\lesssim P_{WTnom}\end{cases} \qquad (6)$$

where α_{WT_i} represents the cost of WT per kW for WT sizes between P_i and P_{i+1}. The annual capital expenses can be calculated as follows:

$$C_{CaWT\_an}=C_{CaWT}/T_{WT} \qquad (7)$$

where T_{WT} is the WT lifetime (years). WT operation expenditure is calculated as follows:

$$OpEx_{\mathrm{WT}}=\mathrm{FCR}\times(C_{CaWT}/T_{WT})+C_{OMWT}E_{WT} \qquad \$/year \qquad (8)$$

where C_{CaWT} is the WT initial cost ($), FCR is the fixed charge rate (interest, insurance, taxes, and others), C_{OMWT} is the WT operation and maintenance cost (O&M) ($/kWh) and E_{WT} is the produced energy (kWh/year)[20],[21]. The first term of Eq. (7) is independent of the WT energy production (insurance, annual interest rate, land leasing, etc.), while the second term is dependent on the WT energy production (parts replacements, production maintenance, etc.). Eq. (7) can be rewritten as follows:

$$OpEx_{\mathrm{WT}}=\mathrm{FCR}(C_{CaWT}/T_{WT})+C_{OM}\sum_{k=1}^{8760}P_{WT}(k) \qquad \$/year \qquad (9)$$

2.2 Solar PV Model

PV represents one of the major renewable energies that achieved significant growth. According to the Solar Energy Industry Association (AEIS) report [22], about 50% of newly electricity-generating capacity added to the US grid in 2022 comes from solar stations. For the fourth year in a row, PV technology came at the top technology for new additions. The PV market grew by more than 95% in the USA. The renewables account for generating +315 GW in 2022, 50% comes from PV [23]. The rapid increase in PV installation is due to the massive production of PV modules from China which produced about 61% of global production in 2016 (about 45000 MW annually). Such a production rate reduced the module cost from $0.65/W in 2015 to $0.39/W in 2016 [22]. The prices were reduced in 2020 to $0.23/W for monocrystalline modules [24]. The selection of PV systems is critical where capital expenditure represents from 75% to 90% of the life cycle cost (the O&M contributes only 10% to 25%) [25].

The output power of the PV module ($P_{PVm}(k)$), at any sample time k, is dependent on ambient irradiance ($P_{irr}(k)$ (kW/m^2)), panel temperature (T), PV area (a_{module}) and PV module efficiency (μ_{PV}) as follows:

$$P_{PVm}(k)=\begin{cases}P_{irr}(k)\times a_{module}\times\mu_{PV}\times D\times\mu_t & P_{irr}(k)\times\mu_{PV}\times a_{module}<P_{PVnom}\\ P_{PVnom}\times\mu_t\times D & P_{irr}(k)\times\mu_{PV}\times a_{module}\ge P_{PVnom}\end{cases} \qquad (10)$$

where P_{PVnom} is the nominal power of the PV module under standard test conditions, D is the annual degradation rate of solar panels, and μ_t is the temperature efficiency factor which can be calculated using the following equation:

$$\mu_t=1-[\Upsilon\times(T-T_{STC})] \qquad (11)$$

where T_{STC} is the Standard Test Conditions temperature, and Υ is the power temperature coefficient (typically 0.005 for crystalline silicon) [9],[26].

The module efficiency (μ_{PV}) can be calculated using the following formula:

$$\mu_{PV}=\frac{P_{PVnom}}{P_{irrSTC}} \qquad (12)$$

where P_{irrSTC} is the irradiance under standard test conditions (1000 W/m^2).

Hence the total generated power of an N_{PV} installed PV module is given by:

$$P_{PV}(k)=P_{PVm}(k)\times N_{PV} \qquad (13)$$

The annual generated energy using PV is given by:

$$E_{PV}=\sum_{k=1}^{8760}P_{PV}(k) \qquad kWh \qquad (14)$$

PV systems are composed of PV modules, inverters, wiring, and other hardware components. The rate of change of prices of PV system components differs. While the price of PV panels changes dramatically, the prices of inverters and other hardware do not. In addition to the components of a PV system, the installation cost is another major parameter in the determination of the capital cost of a PV system. The capital cost of the PV system can be calculated as follows:

$$C_{CaPV}=(C_{mod}+C_{inv}+C_{BOS}+C_{ins})\times P_{PVnom} \qquad (15)$$

where C_{mod} is the module cost, C_{inv} is the inverter cost, C_{BOS} is wiring and other hardware costs (Balance of System) and C_{ins} are the installation expenses per kW rating power of the generator. The annual capital expenses can be calculated as follows:

$$C_{CaPV\_an} = C_{CaPV}/T_{PV} \tag{16}$$

where T_{PV} is the PV lifetime.

The O&M (operational and maintenance) expenditure

$$OpEx_{\mathrm{PV}} = \mathrm{FCR} \times (C_{CaPV}/T_{PV}) + C_{OMPV}E_{PV} \qquad \$/year \tag{17}$$

Where C_{CaPV} is PV initial cost ($), C_{OMPV} is the PV operation and maintenance cost (O&M) ($/kWh), and E_{PV} is the produced energy (kWh/year). Eq. (17) can be rewritten as follows:

$$OpEx_{\mathrm{PV}} = \mathrm{FCR} \times (C_{CaPV}/T_{PV}) + C_{OMPV} \sum_{k=1}^{8760} P_{PV}(k) \quad \$/year \tag{18}$$

Table 2 shows the PV data used for the simulation.

Table 2 PV data [24], [27].

Item	Value
PV efficiency	16%
Degradation	0.4%
PV lifetime	20 years
Module price	0.35 $/W
Inverter price	13 $/Wac
Inverter lifetime	10 years
BOS (Structural and Electrical)	0.4 $/W

2.3 Furnace Model

As a result of low gas prices compared to any other source of energy, furnaces are the first option to produce heat energy. However, the cost of each ton of emission produced by fossil fuel and restrictions by international protocols and agreements concerning the environment may flip the equation in favor of environmentally friendly energy sources. Despite the effort to reduce fossil fuel consumption, they represent a competitive energy source for heat and transportation applications due to low prices and high energy density. In the case study of this paper, in addition to the electrical heater, the furnace is used to satisfy the MEG heat demand.

The capital cost of the furnace (C_{CaFur}) is given by:

$$C_{CaFur} = \alpha_{Fur} \times P_{Furnom} \tag{19}$$

where α_{Fur} is the cost of the furnace per 1kBUT/hr and P_{Furnom} is the nominal power of the installed furnace. α_{Fur} can be calculated as follows:

$$\alpha_{Fur} = \begin{cases} \alpha_{Fur_1} & P_1 \geq P_{Furnom} \\ \vdots & \vdots \\ \alpha_{Fur_i} & P_i \leq P_{Furnom} \leq P_{i+1} \\ \vdots & \vdots \\ \alpha_{Fur_N} & P_N \leq P_{Furnom} \end{cases} \tag{20}$$

where α_{Fur_i} represents furnace initial and installation costs per 1kBUT/hr of furnace size between P_i and P_{i+1}. The annual capital expenses can be calculated as follows:

$$C_{CaFur\_an} = C_{CaFur}/T_{Fur} \tag{21}$$

where T_{Fur} is the Furnace lifetime (years).

Furnace operation expenditure is calculated as follows:

$$OpEx_{\mathrm{Fur}} = \mathrm{FCR} \times (C_{CaFur}/T_{WT}) + C_{fuel} \times C_P \times \sum_{k=1}^{8760} P_{Fur}(k) \times \frac{100}{\mu_{Fur}} + C_{MFur} \times \sum_{k=1}^{8760} P_{Fur}(k) \qquad \$/year \tag{22}$$

where C_{MFur} is the furnace maintenance cost ($/kWh), C_P is the Specific energy (MJ/kg), $C_{fuel}$is the fuel price ($/kg) and μ_{Fur} is the furnace efficiency. The CO_2 emission (kg/ year) is calculated by:

$$m_{co2} = EF_{co2} \times \sum_{k=1}^{8760} P_{Fur}(k) \times \frac{100}{\mu_{Fur}} \tag{23}$$

where EF_{co2} is the CO_2 emission factor.

The furnace requires electrical power $P_{eleFur}(k)$ for its operation is given by:

$$P_{eleFur}(k) = \beta_{eleFur} \times P_{Fur}(k) \tag{24}$$

where $P_{Fur}(k)$ is the current heat rate of the furnace, β_{eleFur} is the electrical coefficient of the furnace dependent on furnace type as given in Table 3 [28].

Table 3 Electrical coefficient for different furnace types

Furnace type	β_{eleFur}
Non-Condensing Furnace	0.000006 kW/Btu/h
Condensing furnace with PSC motor	0.000009 kW/Btu/h
Condensing furnace with BPM motor	0.000005 kW/Btu/h

2.4 Electrical Heater and Transformer Model

A simplified Electrical heater model is used for the simulation. The efficiency of the electrical heater is set to 100% and the capital cost is given by the following equation:

$$C_{CaeleF} = \alpha_{eleF} \times P_{eleFnom} \tag{25}$$

where α_{eleF} is the average capital cost per 1 kBtu/h (set to $35) including the unit price and installation cost. The annual capital expenses can be calculated as follows:

$$C_{CaeleF\_an} = C_{CaeleF}/T_{eleF} \tag{26}$$

where T_{eleF} is the electric furnace lifetime (years).

The transformer capital cost ($C_{CaTrans}$) is given by:

$$C_{CaT} = \alpha_T \times P_{Tnom} \tag{27}$$

where α_{Trans} is the cost of the transformer per 1kWh and $P_{Transnom}$ is the nominal power of installed Transformer. α_{Trans} can be calculated as follows:

$$\alpha_T = \begin{cases} \alpha_{T_1} & P_1 \geq P_{Tnom} \\ \vdots & \vdots \\ \alpha_{T_i} & P_i \leq P_{Tnom} \leq P_{i+1} \\ \vdots & \vdots \\ \alpha_{T_N} & P_N \leq P_{Tnom} \end{cases} \tag{28}$$

where α_{T_i} represents the initial and installation costs of the furnace per 1 kWh of transformer size between P_i and P_{i+1}. The annual capital expenses can be calculated as follows:

$$C_{CaT\_an} = C_{CaT}/T_T \tag{29}$$

where T_T is the transformer lifetime (years). The transformer losses are given by:

$$P_{T_{loss}}(k) = \mu_T P_L(k) \tag{30}$$

where μ_T is the transformer efficiency and $P_L(k)$ is the load power at instance k.

3 Control Algorithm

The control flowchart is shown in Fig. 4. The heat and power control algorithms are identical. The algorithms start by sorting the energy sources based on their operational costs (namely the fuel prices, hence, renewable sources costs are negligible during the sorting process). Then, the algorithms request a supply for the current demand (heat or power) from a source with a lower operational cost.

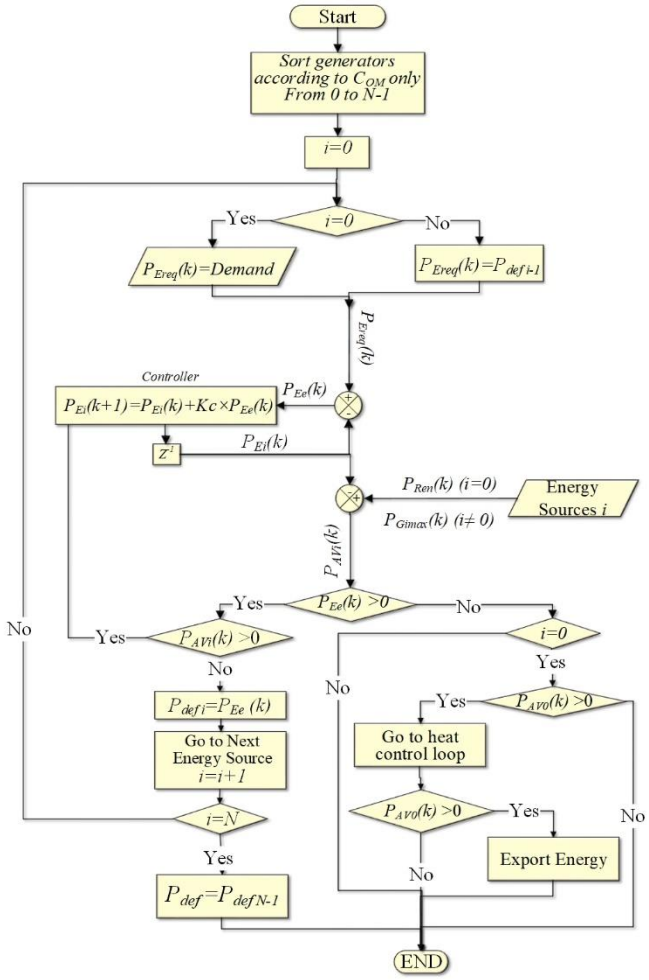

Fig. 4 Control flowchart

The control loop increments the control action dynamically to match the required demand and simultaneously calculate the available power based on both generated power and source capacity according to the following equations:

$$P_{Ee}(k) = P_{Ereq}(k) - P_{Ei}(k) \tag{31}$$

$$P_{Ei}(k+1) = \begin{cases} P_{Gimax} & P_{Ei}(k+1) \geq P_{Gimax} \\ P_{Ei}(k) + K_c \times P_{Ee}(k) & 0 \leq P_{Ei}(k+1) \leq P_{Gimax} \\ 0 & P_{Ei}(k+1) \leq 0 \end{cases} \tag{32}$$

where $P_{Ereq}(k)$ is the required electrical power at instant k, $P_{Ee}(k)$ is the error between currently required power and the delivered power to the load $P_{Ei}(k)$, and P_{Gimax} is the capacity of the generator i. For renewable sources, the equation will be slightly modified to the following:

$$P_{Ei}(k+1) = \begin{cases} P_{Ren}(k) & P_{Ei}(k+1) \geq P_{Ren}(k) \\ P_{Ei}(k) + K_c \times P_{Ee}(k) & 0 \leq P_{Ei}(k+1) \leq P_{Ren}(k) \\ 0 & P_{Ei}(k+1) \leq 0 \end{cases} \tag{33}$$

where $P_{Ren}(k)$ is the generated power from renewables at instant k. If the generated power reaches the capacity limit of the source, the algorithms shift to the next energy source with the next lower operational cost. The process repeats till the load is satisfied or the generated power reaches the full capacity of all generators. The total power deficiency (P_{def}) represents the unfulfilled demand from all given sources.

4 MEG Optimization using Genetic Algorithms

Unlike conventional optimization techniques, GA is a search algorithm that can guarantee a global minimum. Each parameter of the optimization problem is coded in what is called a "Gene". The collection of genes (optimization parameters) forms a chromosome. Individuals in GA are presented by the different settings of the value of the gene and hence the chromosome. Accordingly, everyone is a potential solution. A population of a random set of individuals forms the first generation. The fitness function is a tool to measure how efficient everyone is to be a candidate solution to the problem. According to their fitness, individuals are selected for crossover. Parents and offspring, resulting from the crossover, are used to form the next generation. The process repeats till a significant level of fitness is achieved or the number of generations reaches a predefined value. To avoid getting stuck in the local minimum, a mutation is added to the process. The mutation is the process by which a very low percentage of the genes are exposed to random change. The mutation process forces the search algorithm to skip from the current solution pool to the unexplored area in the search domain. The percentage of crossover and mutation affect the speed of the search process.

The optimization process is performed through two phases. In the first phase, the optimal structure of the supply system is achieved by considering annual capital expenditure, maintenance, and operation (M&O) expenditure, and energy deficiency to form the cost function. The parameters of MEG that are subjected to the optimization process are the sizes of each generator in addition to the required inverters and transformers to connect to loads, grid, and local power station. Hence, the chromosome of everyone is given by:

$$x = [P_{WTnom} \quad P_{PVnom} \quad P_{TRnom} \quad P_{Furnom} \quad P_{eleFurnom}] \tag{34}$$

The fitness function is reciprocal to the cost function as follows:

$$f = \frac{1}{1 + C_I} \tag{35}$$

where C_I is the cost function and is given by:

$$C_I = \eta_1 C_{PPkWh} + \eta_2 C_{E_{def}} \tag{36}$$

where η_1 and η_2 are coefficients representing the significance of each term to the optimization process, C_{PPkWh} is the average price per kWh of electrical or heat energy and is given by:

$$C_{PPkWh} = \frac{C_t}{E_{Dem} - E_{def}} \quad (37)$$

$$E_{Dem} = \sum_{k=1}^{8760} P_e(k) + \sum_{k=1}^{8760} P_h(k) \quad (38)$$

$$C_t = \sum_{i=1}^{N} \left(C_{Ca_{an}i} + OpEx_i\right) + \frac{m_{co2}}{1000} \times C_{CO2} - C_{sell} \sum_{k=1}^{8760} P_{sell}(k)$$

where E_{Dem} is the yearly energy demand, $P_{sell}(k)$ is the sold power at instant k and C_{sell} is the selling price in $ US per kWh, m_{co2} is the emitted CO_2 kg/year, and C_{CO2} is the cost of CO_2 and set to $37 per ton [29].

$C_{E_{def}}$ represents the normalized energy deficiency of electrical and heat energy demand in one year and given by:

$$C_{E_{def}} = \frac{E_{def}}{E_{Dem}} \quad (39)$$

$$E_{def} = \begin{cases} E_{Dem} + \sum_{k=1}^{8760} \left(\sum_{i=1}^{M} P_{Loss}(i,k) - \sum_{i=1}^{N} P_g(i,k) \right) & if > 0 \\ zero\ other\ wise \end{cases} \quad (40)$$

where $P_g(i,k)$ is the generated power from generator i, $P_{Loss}(i,k)$ is the power loss of energy element i in MG at instance k, E_{Dem} is the electrical and heat energy demand in one year and $P_e(k)$, and $P_h(k)$ is the power and heat demand at instance k respectively.

5 Simulation and Results

One-year profiles of heat and power loads for midsize houses [30] are used for the simulation. Those profiles were scaled to fit 200 midsize houses located near the urban Toronto area. The irradiance, temperature, and wind speed profiles at the same location are applied [31].

The GA optimization was performed over eight generations each generation is 60 individuals. Each individual represents a potential solution of the size of all generators and energy conversion technologies used in this simulation. The crossover probability was set to 80% while the mutation was set to 5%. The optimization was conducted for two scenarios, the interest rate in the first scenario was set to zero% while it was set to 5.25% for the second scenario.

5.1 Scenario I

In this scenario, the interest rate was set to zero. Fig. 5 shows the optimization results of the first scenario. As can be noted from Fig. 5(a) the maximum fitness was converged to a solution and was close to 7. Fig. 5(b) shows the progress of KPIs (key performance indices) of the best individual (the terms of the cost function of the optimization) vs. the generations. It confirms the stability optimization process, and that the optimization was almost settled after the sixth generation. Table 4 shows the detailed progress of the optimization by the generations. The first four columns represent the parameters that are subjected to optimization (the sizes of the energy generators), the next four columns represent the terms of the cost function, and the last column represent the fitness value of this individual. The table shows how the optimization algorithm reduces the use of gas over generations due to high emission costs. The price of energy is about 11.4 ₡/kWh in addition to the emission price that should be added (0.1 ₡/kWh), the power deficiency is about 2% and the excessive power is close to zero. The results of the best individual over a generation are listed in Table 4.

Table 4 Results of optimization over generations (first scenario interest rate = 0.0%)

Generation	WT (kW)	PV (kW)	Transformer (MW)	Furnace (kW)	Price ($/kW)	Emission Cost ($/kW)	E_def ratio	E_excess ratio	Fitness
1	6032	3692	5	21564	0.194	0.097	0.020	0.009	3.120
2	572	3691	5	21564	0.110	0.086	0.020	0.000	4.625
3	270	3217	6	1105	0.099	0.044	0.020	0.000	6.145
4	1900	3216	6	6	0.140	0.000	0.021	0.000	6.211
5	270	3832	4	970	0.105	0.038	0.021	0.000	6.096
6	270	3831	7	35	0.122	0.001	0.021	0.000	6.943
7	170	3216	6	27	0.116	0.001	0.021	0.000	7.262
8	100	3216	6	26	0.114	0.001	0.021	0.000	7.345

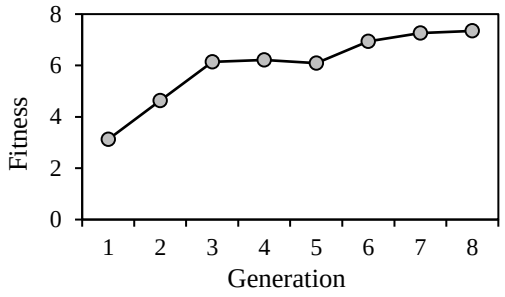

(a)

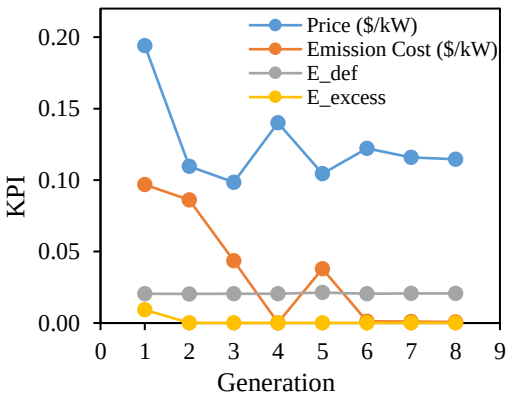

(b)

Fig. 5 Optimization results for 1st scenario (a) Fitness VS generations (b) KPIs of best individual vs. generation

Fig. 6 shows the energy consumption from different sources vs. time for the optimized structure of the MEG. It also indicates exported and sold energy from renewables to the grid.

Fig. 7 shows the load contribution percentage from different energy sources of optimized MEG for (a) total load (heat and power), (b) heat load, and (c) power load. It shows that around 61% of the supply is satisfied using reliable sources (grid). It also shows that renewables contribution with significant share in total energy required for heat and power loads (20%). Most of the renewable energy go to power load. The renewable sources contribution for heat and power loads is 7% in addition to 14% exported energy to the grid (the percentage of exported energy is calculated based on the total required energy not the generated one).

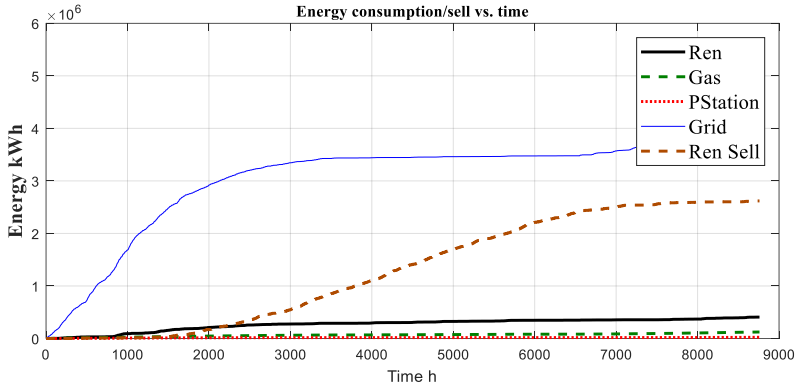

Fig. 6 Energy consumption from different sources vs. time (1st scenario)

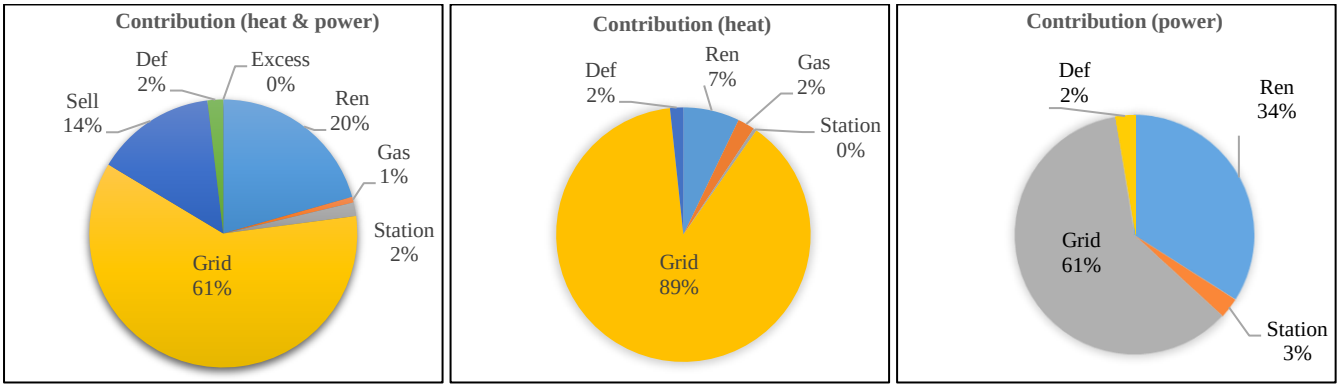

(a) (b) (c)

Fig. 7 Contribution percentage of different energy sources (1st scenario) to (a) total load (heat and power), (b) heat load, and (c) power load. Scenario I (Interest rate is set to zero)

Fig. 8 shows the prices of energy from each source (considering the initial and running cost), the total average cost, and the carbon dioxide cost.

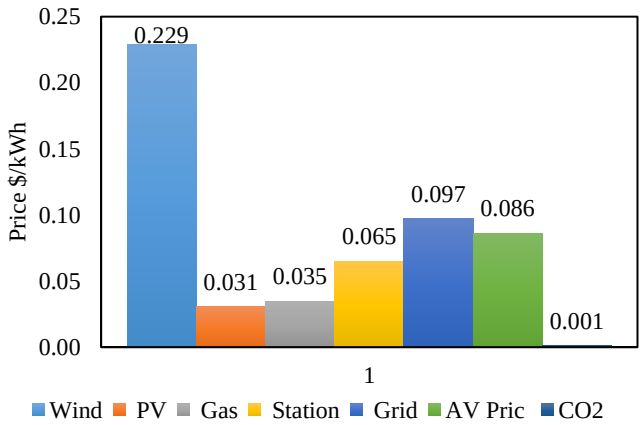

Fig. 8 Energy prices for 1st scenario (interest rate is set to zero)

PV recorded the minimum kWh cost; however, the optimization process didn't favor PV over the conventional energy sources (grid).This is because of the mismatch between the PV energy generation profile and the load profile in addition to a large gap between selling and buying prices from and to the grid (sell price set to 2.5 cents while grid energy price ranges from 8-12 cents). Hence, any increase in PV size would have a negligible effect on the prices of consumed energy per kWh. The figure also indicates that the prices of energy generated by wind turbines are very high. This is due to its high initial cost. However, the wind energy profile has less mismatch with the load profile than PV. Accordingly, wind turbines were among the energy technologies of optimized MEG. It should be noted that the emission cost per kWh is referred to the total generated energy from all sources. Hence, with low share of the furnace in the system, this figure is very small.

5.2 Scenario II

An additional scenario was performed to address the impact of the high initial cost of energy technology on the structure of the optimal MEG by setting high-interest rates (5.25%). It also addresses the effect of high-interest rates on the progress of renewables in any power system. Fig. 9 shows the optimization results of the second scenario as discussed in the first scenario. The results of the best individual over a generation are listed in Table 5. The table shows how the optimization algorithm reduces the use of renewables over generations due to the high interest rates. The lag of renewables was compensated by the grid and the gas. However, the fitness of the fifth generation is very close to the eighth generation with higher share of renewables (note that the total cost of kWh is the addition of the kWh price plus the emission cost).

Table 5 Results of optimization over generations (second scenario, interest rate = 5.25%)

Generation	WT (kW)	PV (kW)	Transformer (MW)	Furnace (kW)	Price ($/kW)	Emission Cost ($/kW)	E_def ratio	E_excess ratio	Fitness
1	6032	3692	5	21564	0.245	0.040	0.020	0.009	3.181
2	572	3691	5	21564	0.129	0.062	0.020	0.000	4.742
3	270	3217	6	1105	0.111	0.036	0.020	0.000	5.963
4	550	3699	3	1105	0.124	0.035	0.029	0.001	5.302
5	270	3866	6	334	0.130	0.010	0.020	0.000	6.201
6	572	3516	9	829	0.128	0.026	0.020	0.000	5.729
7	297	3806	4	6	0.137	0.000	0.032	0.000	5.883
8	407	25	8	829	0.093	0.029	0.020	0.000	7.002

Fig. 9(b) shows that the KPIs are kept nearly the same. The energy consumption from renewable sources was reduced compared with scenario I as can be noted in Fig. 10. Fig. 11 presents a full image of the impact of high-interest rates on MEG structure. It shows that the renewables contribution shrinks to 2%. The gas and grid contribution increased significantly (93%). Fig. 12 presents the prices of energy kWh generated by each technology. The PV kWh prices went higher than first scenario. The contribution of the privet station in both scenarios is the same. This is due to the limited power offered by the station. However, it also indicates the importance of additional sources that can reduce the mismatch between generation and demand profiles.

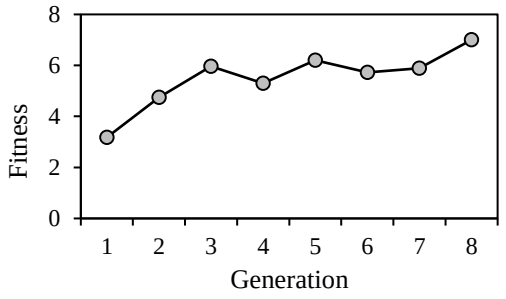

(a)

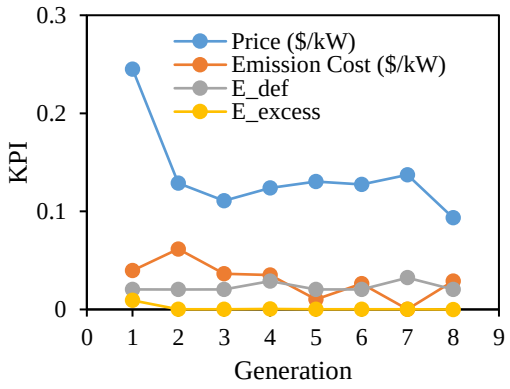

(b)

Fig. 9 Optimization results for 2nd scenario (a) Fitness VS generations (b) KPIs of best individual vs. generation

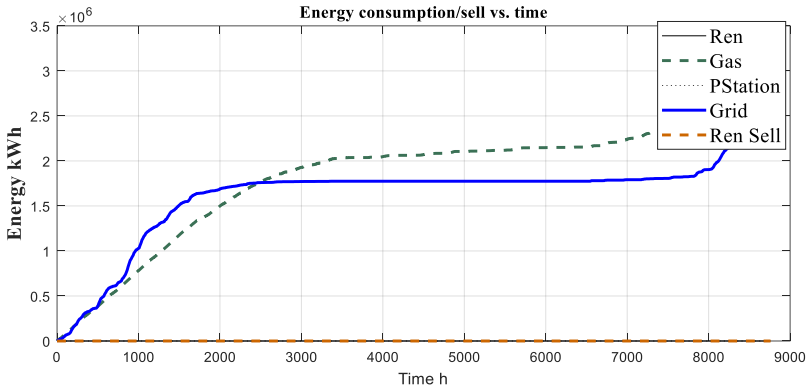

Fig. 10 Energy consumption from different sources vs. time (2nd scenario)

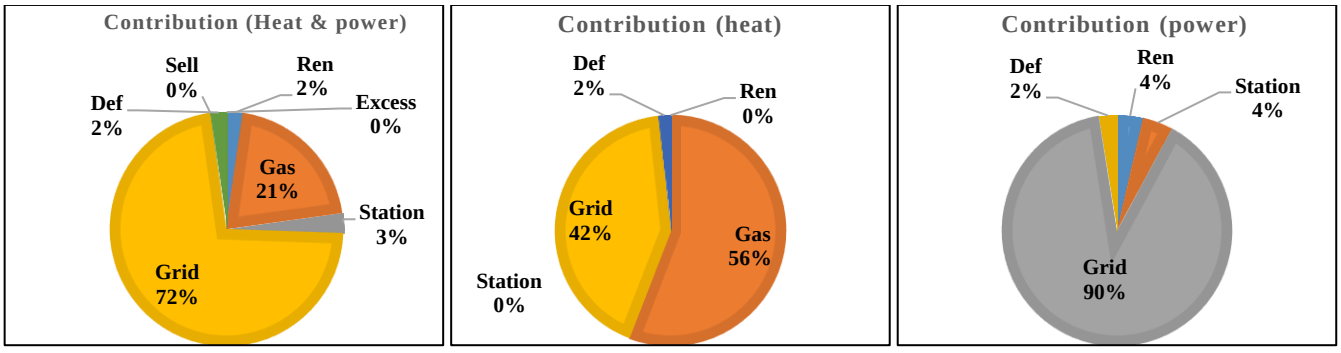

(a) (b) (c)

Fig. 11 Contribution percentage of different energy sources (2nd scenario) to (a) total load (heat and power), (b) heat load, and (c) power load. Scenario II (Interest rate is set to 5.25%)

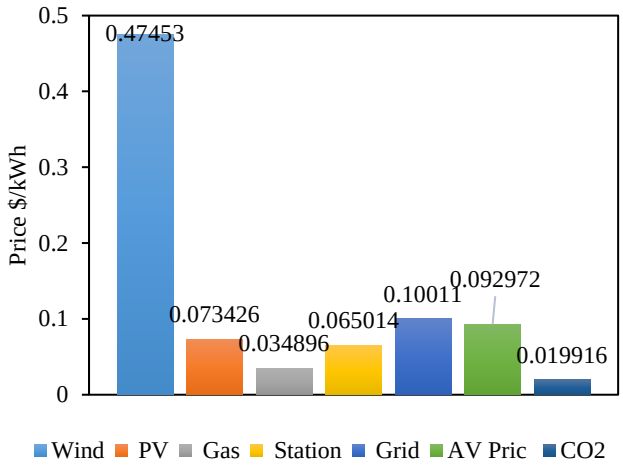

Fig. 12 Energy prices for 2nd scenario (interest rate is set at 5.25%)

Fig. 13 shows the system response for the heat power by applying the two control loops with algorithms presented in section 4. It shows how the control loops ensures close matching between the demand and supply. The control algorithms are applied during the optimization process which insures optimal structure and operation.

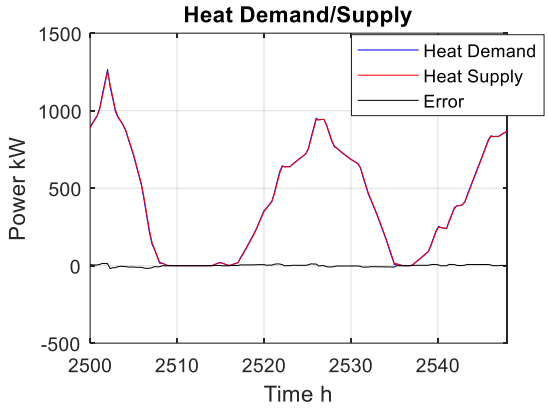

(a)

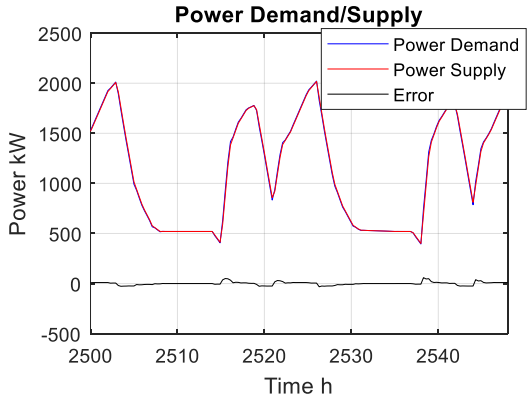

(b)

Fig. 13 The control system response (a) for heat control loop and (b) for power control loop

Table 6 represents the size of each energy technology resulting from the optimization process for the different scenarios.

Table 6 Result of optimization for different scenarios

Scenario	I	II
Total WT size (kW)	100	407
Total size PV (kW)	3215.5	24.75
Furnace (kBtut/h)	88	2830
Grid Transformer size (kW)	5000	4000

6 Conclusions

In this paper, an optimization process to the structure of MEG in grid-connected mode is performed. The optimization objective focused on minimizing cost, carbon dioxide emission, and energy deficiency. The optimized structure was subjected to a scheduling algorithm that guarantee low-price operation considering the availability. In addition, closed-loop feedback operation using a PI controller is implemented at a low control level for both heat and power loops. The control loops guarantee dynamic matching between the demand profile and the supply profile. The results of the optimization and operation of the MEG are presented in two scenarios. The first scenario considers 0% interest rates while the second scenario presents 5.25% interest rates. The results show that due to the high initial prices of renewables (especially WT), their contribution is reduced due to the high-interest rates. In addition, the mismatch between the renewables production profile and load profile, as well as, the low exporting tariff, have a negative impact on renewables' share in the power system. This is evident when we compare the low LCOE for PV with other sources used in this work. Moreover, the addition of a carbon tax effectively reduces the share of gas as a source of energy.

References

[1] Eckhart M., El-Ashry M., Hales D., Hamilton K., and Rae P., 2020 "Renewables, Global Status report," REN21.

[2] Eckhart M., El-Ashry M., Hales D., Hamilton K., and Rae P., 2018 "Renewables, Global Status report," REN21.

[3] "Summary Report: 2012 DOE Microgrid Workshop.," 2012.

[4] Parhizi, S., Lotfi, H., Khodaei, A. and Bahramirad, S., 2015. State of the art in research on microgrids: A review. IEEE access, 3, pp.890-925.

[5] Ma, T., Wu, J. and Hao, L., 2017. Energy flow modeling and optimal operation analysis of the micro energy grid based on energy hub. Energy conversion and management, 133, pp.292-306.

[6] Gabbar, H.A. and Zidan, A., 2016. Optimal scheduling of interconnected micro energy grids with multiple fuel options. Sustainable Energy, Grids and Networks, 7, pp.80-89.

[7] Han, Y. and Shen, P., 2014. Modeling, control and electromagnetic transient simulation of the doubly fed induction generator-based wind energy generation system. Simulation, 90(3), pp.275-289.

[8] Katzenbach, R., Clauss, F. and Zheng, J., 2015, May. Potentials of sustainable energy management in buildings. In 2015 5th International Youth Conference on Energy (IYCE) (pp. 1-7). IEEE.

[9] Luque, A. and Hegedus, S. eds., 2011. Handbook of photovoltaic science and engineering. John Wiley & Sons.

[10] Jiang, X. and Xiao, C., 2019. Household energy demand management strategy based on operating power by genetic algorithm. IEEE Access, 7, pp.96414-96423.

[11] Raghavan, A., Maan, P. and Shenoy, A.K., 2020. Optimization of day-ahead energy storage system scheduling in microgrid using genetic algorithm and particle swarm optimization. Ieee Access, 8, pp.173068-173078.

[12] Teo, T.T., Logenthiran, T., Woo, W.L., Abidi, K., John, T., Wade, N.S., Greenwood, D.M., Patsios, C. and Taylor, P.C., 2020. Optimization of fuzzy energy-management system for grid-connected microgrid using NSGA-II. IEEE transactions on cybernetics, 51(11), pp.5375-5386.

[13] Moghaddam, A.A., Seifi, A., Niknam, T. and Pahlavani, M.R.A., 2011. Multi-objective operation management of a renewable MG (micro-grid) with back-up micro-turbine/fuel cell/battery hybrid power source. energy, 36(11), pp.6490-6507.

[14] Díaz, G., Planas, E., Andreu, J. and Kortabarria, I., 2015. Joint cost of energy under an optimal economic policy of hybrid power systems subject to uncertainty. Energy, 88, pp.837-848.

[15] Zare, M., Niknam, T., Azizipanah-Abarghooee, R. and Ostadi, A., 2016. New stochastic bi-objective optimal cost and chance of operation management approach for smart microgrid. IEEE Transactions on Industrial Informatics, 12(6), pp.2031-2040.

[16] Kouloura, T.C., Genikomsakis, K.N. and Protopapas, A.L., Systemic assessment of measures for sustainable energy management in buildings: The case of a student dormitory, ECOS2006, Crete-Greece, July 2006. In Conference Proceedings (pp. 861-868).

[17] Zidan, A., Gabbar, H.A. and Eldessouky, A., 2015. Optimal planning of combined heat and power systems within microgrids. Energy, 93, pp.235-244.

[18] International Energy Agency, 2022. Renewable Energy Market Update: Outlook for 2022 and 2023. OECD Publishing.

[19] Spertino, F., Di Leo, P., Ilie, I.S. and Chicco, G., 2012. DFIG equivalent circuit and mismatch assessment between manufacturer and experimental power-wind speed curves. Renewable Energy, 48, pp.333-343.

[20] Wiser, R.H. and Bolinger, M., 2019. 2018 wind technologies market report.

[21] Siyal, S.H., Mentis, D. and Howells, M., 2016. Mapping key economic indicators of onshore wind energy in Sweden by using a geospatial methodology. Energy conversion and management, 128, pp.211-226.

[22] Davis M., Sylvia L.M., Zoe G., Sagar C., Caitlin C., Matthew S., Matt I., Elissa P., and Chris S., "Solar Market Insight Report 2022 Year in Review," Solar Energy Industries Association (SEIA), Washington,, 2022.

[23] REN21, P.R.S., 2022. Renewables 2022 global status report. Renewable Energy Policy Network for the 21st Century (REN21).

[24] Feldman, D., Ramasamy, V., Fu, R., Ramdas, A., Desai, J. and Margolis, R., 2021. US solar photovoltaic system and energy storage cost benchmark (Q1 2020) (No. NREL/TP-6A20-77324). National Renewable Energy Lab.(NREL), Golden, CO (United States).

[25] Tjengdrawira, C. and Richter, M., 2016. Review and Gap Analyses of Technical Assumptions in PV Electricity Cost Report on Current Practices in How Technical Assumptions Are Accounted in PV Investment Cost Calculation. No. Solar Bankability WP3 Deliverable D, 3.

[26] Ufluoğlu, E.E. and Kayakutlu, G., 2016. Mathematical model for a microgrid consisting of wind turbine, PV panels, and energy storage unit. Journal of Renewable and Sustainable Energy, 8(5).

[27] Feldman, D., Ramasamy, V., Fu, R., Ramdas, A., Desai, J., and Margolis, R., 2021. U.S. Solar Photovoltaic System Cost Benchmark: Q1 2020. Golden, CO: National Renewable Energy Laboratory. NREL/TP-6A20-77324.

[28] How much does it cost to install an electric furnace? Fixr.com | Electric Furnace Cost | Electric Furnace Replacement Cost. Available at: https://www.fixr.com/costs/electric-furnace.

[29] Canada, E. and C.C. (2021) Government of Canada, Canada.ca. Available at: https://www.canada.ca/en/environment-climate-change/services/climate-change/pricing-pollution-how-it-will-work/industry/pricing-carbon-pollution.html.

[30] "Heating with electricity," Natural Resources Canada's, Office of Energy Efficiency, 2003. https://natural-resources.canada.ca/sites/www.nrcan.gc.ca/files/energy/pdf/energystar/Heating_with_Electricity.pdf

[31] NSRDB. Available at: https://nsrdb.nrel.gov/.